energy&fuels

pubs.acs.org/EF

Article

Well-to-Wheel Design of Renewable Fuels for Future Spark-Ignition Engines

Published as part of Energy & Fuels special issue "Celebrating Authors of Energy and Fuels Most-impactful Articles (2023)".

Philipp Ackermann, Marian Panofen, Patrick Burkardt, Bastian Lehrheuer, Jörn Viell, Stefan Pischinger, Alexander Mitsos, and Manuel Dahmen*

Cite This: *Energy Fuels* 2026, 40, 4207−4215

Read Online

ACCESS | Metrics & More | Article Recommendations | Supporting Information

ABSTRACT: Well-to-wheel (WTW) performance is an important metric for alternative fuels. Current methods for model-based fuel design optimize either the well-to-tank (WTT) or the tank-to-wheel (TTW) performance, and address the respectively other aspect only indirectly, e.g., via simple approximations, if at all. To enable WTW fuel design, we combine a superstructure-based WTT fuel design method with a TTW model that estimates achievable engine efficiencies with a dynamic, zero-dimensional engine model. For computational tractability, we approximate the engine model with an artificial neural network as surrogate model. We then design alternative fuels with optimal WTW performance. We find that aiming at very strong TTW performance by means of an aggressive constraint on the research octane number can impair the WTW performance. Alternative fuels for tailored engines offer significantly more flexibility in terms of fuel components and production processes and thus potential for cost and global warming impact reductions than drop-in fuels designed with the same superstructure. The findings emphasize the importance of addressing the entire life cycle of a fuel at early stage design.

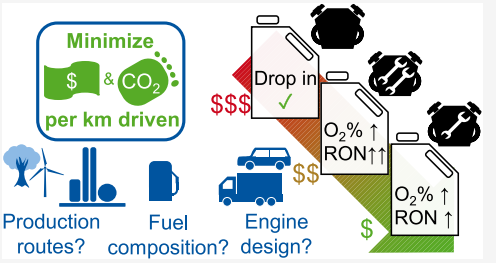

INTRODUCTION

The usage of fuels produced from renewable resources in internal combustion engines can contribute to the mitigation of climate change. Prominent renewable fuels include methanol[1−4] and ethanol.[1,5] These light alcohols exhibit a low autoignition propensity and hence a high knock resistance. They can therefore be used in spark-ignition (SI) engines that use higher boost pressures and compression ratios than the gasoline-fueled engines currently in the market.[3,5] Such advanced SI engines achieve higher thermodynamic efficiencies, providing a lever to reduce the overall cost and environmental impact of a fuel.[6,7] The promise of engine efficiency improvements has prompted the development of fuel design methods that aim at co-optimizing renewable fuels and engines.[8,9]

Model-based fuel design identifies potential fuel molecules, see, e.g.,[10] optimal mixture compositions, see, e.g.,[11] or both, see, e.g.,[12] Since advanced SI engines require fuels with high knock resistance,[13] fuel design typically targets autoignition indicators like the research octane number (RON). Knock-resistant fuels can be either designed by defining restrictive constraints on autoignition indicators[8,9] or by optimizing the autoignition indicator value of the fuel.[10,14] While autoignition indicators and achievable engine efficiency are correlated,[15] more targeted approaches optimize the tank-to-wheel (TTW) performance using an engine model to predict fuel-dependent engine efficiency performance.[16,17] While the TTW performance influences the WTW performance, the well-to-tank (WTT) performance must also be considered to optimize the WTW performance.

To address the WTT performance, model-based fuel design has been combined with production pathway optimization using the notion of superstructures. Early approaches use mass balances of reaction networks,[18−20] which allow optimization of simple production metrics such as resource efficiency. More detailed WTT fuel design approaches utilize superstructures that contain more detailed process information from thermodynamically sound shortcut methods[21] or even rigorous process simulations[22] and thus enable the optimization of large-scale production cost and global warming impact (GWI) of a fuel.

To indirectly address TTW performance, WTT design of SI engine fuels includes constraints on the RON.[20,23] However,

Received: November 5, 2025
Revised: January 26, 2026
Accepted: January 27, 2026
Published: February 12, 2026

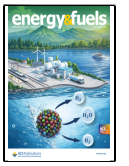

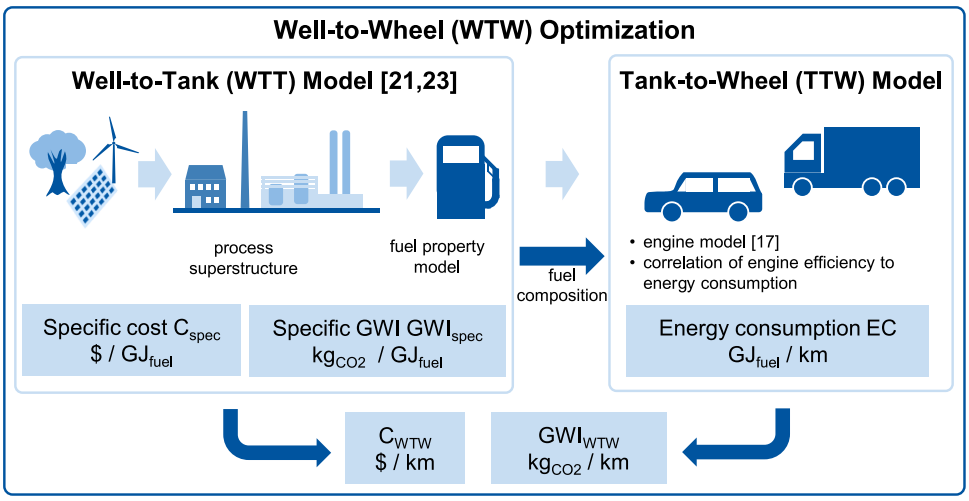

Figure 1. Well-to-wheel (WTW) optimization approach: We take the well-to-tank (WTT) model from König et al.[21,23] and extend it by the tank-to-wheel (TTW) model described in this section.

minimum RON requirements may reduce the design space, potentially excluding WTW-optimal fuels that have rather low RON but excellent production performance. To find WTW-optimal fuels, a holistic approach considering production and combustion simultaneously is required. A first step toward WTW optimization has been taken by Zhang and Sarathy,[24] who optimized the carbon footprint of blends of fossil gasoline with biobased ethanol, considering the design of the production facilities as well as the TTW emissions. In particular, the TTW emissions account for a possible engine efficiency increase enabled by higher ethanol contents, utilizing a polynomial correlation fitted to experimental engine data.[25] Due to its reliance on experimental engine data, the approach by Zhang and Sarathy[24] is, however, not applicable to a broader range of alternative fuel constituents.

To overcome the limitations of existing fuel design methods, we propose a WTW fuel design method combining our WTT fuel design[21] and a TTW model that is based on a dynamic, zero-dimensional engine model[17] that was validated for different alternative fuels and engine configurations. To incorporate the engine efficiency calculated with the engine model into the nonlinear optimization problem, we derive an artificial neural network (ANN) surrogate model for the engine model. We apply our new method to a process superstructure containing mainly selective conversion routes to oxygenated and nonoxygenated hydrocarbons.

The remainder of the article is structured as follows. The following section describes the overall WTW optimization formulation, and the newly derived WTT model, including the development of the engine surrogate model and the correlation of engine efficiency with fuel consumption. We introduce a case study based on possible fuel constituents, a process superstructure, and fuel specifications. We then design WTW-optimal fuels with different RON requirements and evaluate their performance. Subsequently, we benchmark the results against drop-in fuels designed with the same process superstructure.

WELL-TO-WHEEL FUEL DESIGN

Figure 1 shows an overview of the proposed WTW fuel design method. We extend our previously published method for WTT design[21,23] with the TTW model described in this section. In these references, the WTT model calculates the specific cost of the fuel C_{spec} and the specific GWI of the fuel GWI_{spec} in relation to the lower heating value of the fuel. In order to quantify the impact of engine efficiency improvements enabled by alternative fuels, we herein calculate both the WTW cost of the fuel C_{WTW} and the WTW GWI of the fuel GWI_{WTW} in relation to the distance driven. For this purpose, we consider the energy consumption EC, which gives the energy required per kilometer driven.[26] EC relates the WTW performance metrics to the WTT performance metrics in the following manner

$$C_{WTW} = C_{spec} \cdot EC \quad (1)$$

$$GWI_{WTW} = GWI_{spec} \cdot EC \quad (2)$$

We correlate EC to the thermodynamic engine efficiency, which in turn is a function of the fuel composition and the engine design and operation. To estimate the achievable engine efficiency η, we use our recently developed 0D thermodynamic engine model[17] of a single-cylinder research engine. While 0D engine models are usually derived for a fixed fuel and engine design, our model was derived for the purpose of fuel design and therefore captures the influence of the fuel on engine performance.

The extension to WTT optimization is challenging in terms of mathematical problem formulation and choice of optimization solver. On its own, the WTT optimization constitutes a NLP and is solved with the deterministic global solver BARON.[27] The engine model contains ordinary differential equations and integrals. Thus, the direct integration of the engine model into the WTW optimization would either require fully discretizing the engine model or using a dynamic optimization solver, in contrast to the NLP solver for the WTT. However, the WTW fuel design does not require explicit information about the time-dependent thermodynamic states, but only about the overall engine performance. This motivates the use of a surrogate model based on ANN that predicts the required engine performance as a function of fuel composition and engine configuration. In contrast to the dynamic engine model, the ANN can be integrated efficiently into the algebraic WTT model, obtaining a hybrid mechanistic/data-driven WTW model.[28]

https://doi.org/10.1021/acs.energyfuels.5c05792
Energy Fuels 2026, 40, 4207−4215

Tank-to-Wheel Model

The engine model[17] predicts the net indicated efficiency η as a function of molar fuel composition $\boldsymbol{z}$, the compression ratio ε_{CR}, and the intake pressure p_{in}. When including the engine model in a mathematical optimization, both the knock occurrence k_I[29] and the peak pressure p_{peak} need to be constrained to ensure safe engine operation, i.e., to avoid the occurrence of knock and to avoid exceeding the peak pressure limit

$$\begin{aligned} k_I &\leq 0.99 \\ p_{peak} &\leq 200\ \text{bar} \end{aligned} \tag{3}$$

Hence, the engine model can be replaced with an ANN surrogate model f that gives the input-output relationship

$$\begin{bmatrix} \eta \\ \log k_I \\ p_{peak} \end{bmatrix} = f(\boldsymbol{z}, \varepsilon_{CR}, p_{in}) \tag{4}$$

where the inputs constitute the vector containing the mole fractions of the fuel constituents in the fuel $\boldsymbol{z}$, the compression ratio ε_{CR}, and the intake pressure p_{in}; the outputs constitute the engine efficiency η, the logarithm of k_I,[29] and p_{peak}. Note that the surrogate model does not require fuel properties as an explicit input. In the engine model, the fuel properties are calculated as a function of the fuel composition.

To calculate the fuel consumption in a driving situation, a vehicle model that determines the required engine loads and simulates the different loads for each fuel and engine configuration would be needed. Lacking such a model, we pragmatically assume an inversely proportional correlation between the energy consumption EC and the peak engine efficiency η, using a reference energy consumption EC_{ref} and a reference peak efficiency η_{ref}:

$$EC = \frac{EC_{ref}\eta_{ref}}{\eta} \tag{5}$$

As reference we consider conventional gasoline, using an energy consumption from a real driving scenario[26] EC_{ref} = 2.3 MJ km^{-1} and a peak efficiency of 38.9%, which is the maximum achievable engine efficiency for gasoline in our engine model. Obviously, this correlation is a gross simplification of the actual relation between peak efficiency and fuel consumption.

Overall Optimization Problem

We solve the following optimization problem:

$$\min \begin{bmatrix} C_{WTW} \\ GWI_{WTW} \end{bmatrix}$$

s.t. **Well-to-tank model [21, 23, 30]**

Process superstructure,

Fuel property model

Tank-to-wheel model

ANN surrogate for the engine model (4),

Engine safety constraints (3),

Correlation of engine efficiency to energy consumption (5)

The biobjective optimization problem is implemented in GAMS[31] by including the equations of the TTW model in our previous WTT implementation.[23,30] The ANN surrogate is written in full-space formulation, i.e., the optimizer sees variables and equations corresponding to the neurons.[28] We solve the optimization problem using the ε-constraint method[32] and the deterministic global solver BARON version 22.2.3[27] with the local NLP solver CONOPT 4.1.[33] The relative optimality tolerance is set to 0.01, the maximum CPU time is set to 600 s for each Pareto point. Like König et al.[23] and Panofen et al.,[30] we observe that the value of the upper bound does not decrease after preprocessing, and the value of the lower bound increases only within the first few iterations.

While BARON cannot prove convergence to optimality within the desired tolerance, we refrain from increasing the maximum CPU time in order to not increase computational effort. Convergence in the desired time could potentially be achieved by changing the formulation of the optimization problem and/or employing a different solver. In particular, our global deterministic MINLP solver MAiNGO[34] has outperformed BARON in process design problems using reduced space formulations[35] and performs especially well in solving problems with ANN-based surrogate models.[36] However, applying MAiNGO efficiently for the WTW optimization would require deriving a reduced-space formulation for the WTT model which would require a disproportionate manual effort and likely not lead to significant improvements—if any—in the solution.

RENEWABLE FUELS FOR ADVANCED SPARK-IGNITION ENGINES

Fuel Constituents, Process Superstructure, and Fuel Specifications

We build on our previous study on WTT design of SI engine fuels,[23] in which we optimized C_{spec} and GWI_{spec} of fuels for three different fuel specifications derived from the European E10 gasoline standard,[37] the European E85 gasoline standard[38] (for flex fuel vehicle engines (FFVEs)), and requirements of advanced ultrahigh efficiency SI engines (UHEE).[23] Contrary to the previous study, we now consider a fully renewable utility system, following.[30] Furthermore, we exclude fossil gasoline as a blending option to design fully renewable fuels.

In our previous study,[23] optimal fuels with an oxygen content limitation as in the European E10 gasoline standard performed badly in terms of cost and GWI. A possible explanation for these results is the exclusive focus of the employed process superstructure on synthesis routes that produce single-species products with rather high selectivity.[23] It could be more promising to produce renewable drop-in fuels via synthesis routes to hydrocarbon mixtures, most notably, the Methanol-to-Gasoline (MtG)[39] and the Fischer–Tropsch (FT)[40] process. The inclusion of these routes into our superstructure, however, is not straightforward. Our superstructure was developed for the early stage evaluation of rather selective reaction pathways.[41]

In the current study, we include MtG in the process superstructure as a benchmark for synthetic drop-in fuels, using energy demands from conceptual process design studies[42,43] and a gasoline surrogate for the product mixture.[44] Details on the modeling of the MtG process are given in the Supporting Information. We refrain from including FT, since FT generally yields a broader product spectrum that includes fractions more suited to jet and diesel fuel applications. However, the coproduction of fuels for different applications is outside of

https://doi.org/10.1021/acs.energyfuels.5c05792
Energy Fuels 2026, 40, 4207−4215

the scope of this study. Furthermore, the gasoline fraction in FT requires extensive refining to increase its octane number.[45]

We reduce the number of possible fuel constituents and production processes compared to König et al.[23] since in a previous study that quantified the effects of model and data uncertainty many fuel constituents were unlikely to appear in quantities greater than 1 wt % in the Pareto-optimal solutions.[30] Specifically, we apply the Monte Carlo sampling approach described in[30] to the process superstructure and all three fuel specifications to identify species and processes for reducing the size of the superstructure. Given the computational effort, we compute 5 Pareto points per scenario with the ε-constraint method[32] as in,[30] changing the constraint in 25% increments between minimum and maximum GWI. We retain all fuel constituents that have an average mass fraction of ≥5 wt % in at least one Pareto-optimal blend (see Table 1) as well as all the processes that can possibly produce these fuel constituents. The other fuel constituents are discarded, along with the intermediates and production processes only needed to produce the discarded fuel constituents. The resulting reduced superstructure is shown in Figure S1 in the Supporting Information.

Table 1. Possible Fuel Constituents Selected for the Case Study Ordered by Molecule Class[a]

molecule class	fuel constituents
hydrocarbon	cyclopentane, gasoline (MtG), *n*-hexane, 1-hexene, *n*-pentane, toluene
alcohol	ethanol, methanol
ester	ethyl acetate, methyl acetate
ether	2-methyltetrahydrofuran
ketone	2-butanone, 3-pentanone

[a]"Gasoline (MtG)" refers to a synthetic hydrocarbon mixture obtained from the methanol-to-gasoline (MtG) process.

Table 2. Fuel Specifications for Ultra-High Efficiency Engines (UHEEs) and Drop-In Fuels (Reproduced From,[23] Except for the Ethanol, Methanol, and Ether Content)[a]

	UHEE		drop-in (E10)	
property	min	max	min	max
research octane number, RON	110	(150)	95	(150)
motor octane number, MON	(50)	(150)	85	(150)
liquid density at 15 °C (kg m^{-3})	(600)	(2000)	720	775
olefin content (vol %)	(0)	18	(0)	18
aromatic content (vol %)	(0)	35	(0)	35
ethanol content (vol %)	(0)	(100)	(0)	10
methanol content (vol %)	(0)	(100)	(0)	3
ether (5 or more carbon atoms) content (vol %)	(0)	(100)	(0)	22
oxygen content (wt %)	10	(100)	0	3.7
bubble point pressure at 37.8 bar (kPa)	35	100	45	100
mole fraction evaporated at 70 °C (mol %)	3	52	22	52
mole fraction evaporated at 100 °C (mol %)	46	(100)	46	72
mole fraction evaporated at 150 °C (mol %)	75	(100)	75	(100)
surface tension at 25 °C (mN m^{-1})	(0)	30	(0)	(60)
kinematic viscosity at 25 °C (mm^2 s^{-1})	0.5	2	(0)	(100)
enthalpy of vaporization at 25 °C (kJ kg$_{air}^{-1}$)	(0)	60	(0)	(200)

[a]The values in parentheses represent generic constraints introduced for numerical reasons.

We use the UHEE fuel specifications from our previous study[23] (see Table 2). The UHEE fuel specifications adopt a bubble point pressure constraint from the Reid vapor pressure requirement found in the European E85 standard.[38] The requirements on the distillation curve are derived from a typical E85 fuel.[46] The olefin and aromatic contents are taken from the European E10 standard.[37] The UHEE fuel specifications furthermore contain limits on enthalpy of vaporization, viscosity, surface tension, and oxygen content, aiming at facilitating in-cylinder mixture formation and thus reducing the formation of pollutants.[20] The high RON requirement (RON ≥ 110) aims at low autoignition propensity and thus highly efficient combustion. We furthermore design drop-in fuels, using the fuel specifications from König et al.[23] that were derived from the European E10 standard.[37] We furthermore add restrictions on the content of methanol, ethanol, and ethers containing 5 or more carbon atoms based on the E10 standard. We omit specific restrictions with respect to other alcohols and ethers as such components are not present in our case study.

Engine Surrogate Model

To train the engine surrogate model, we sample the input space uniformly during training data generation via an equidistant grid. For the fuel composition, we consider every possible ternary blend and discretize the mole fractions from 0 to 1 with increments of 0.2. For the engine parameters, we consider compression ratios between 8 and 20 with increments of 1.5 and intake pressures between 1 and 2 bar with increments of 0.125 bar. We simulate the engine for every possible input combination to generate the training data. Blends including four constituents or more are not considered to limit the computational effort. All input and output variables are normalized to an interval between −1 and 1 before ANN training.

The obtained simulation data is split into training, validation, and test data with a ratio of 0.7:0.15:0.15. The case study described below contains 13 fuel constituents, resulting in 15 input neurons for the ANN. We choose an ANN architecture with one hidden layer containing 24 fully connected neurons and the hyperbolic tangent function as activation function. The ANN is trained in Matlab[47] using the Levenberg−Marquardt algorithm. The resulting errors of the test set lie within the orders of magnitude of 1×10^{-10} for η, 1×10^{-4} for k_l, and 1×10^{-3} bar for p_{peak}. Because the training data contains blends with up to 3 fuel constituents only, we create a second test set where up to 13 different species can appear in a blend. The errors on this multicomponent test set are comparable to those on the test set with up to 3 fuel constituents, i.e., the ANN can extrapolate successfully to multicomponent blends. Further details are given in the Supporting Information. Since the errors are smaller than the presumed uncertainty of the engine model,[17] we refrain from a systematic hyperparameter optimization.

Results: Influence of RON Restriction on Well-to-Wheel Performance

In previous WTT design studies,[20,23] the TTW performance was only indirectly considered by placing a lower limit on the RON. However, enforcing a RON ≥ 110 might impact WTT

https://doi.org/10.1021/acs.energyfuels.5c05792
Energy Fuels 2026, 40, 4207−4215

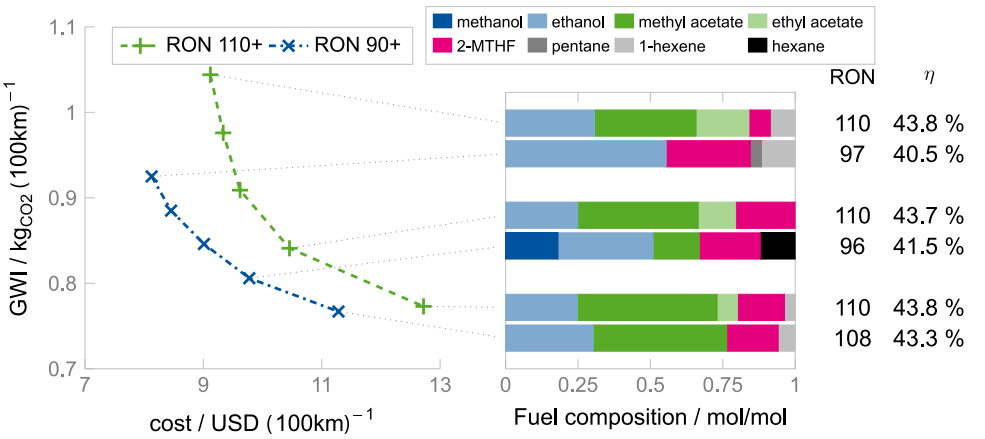

Figure 2. Comparison of well-to-wheel optimized UHEE fuels with different minimum RON requirements. The predicted RON and efficiency η are stated on the right.

performance to an extent that cannot be compensated by superior TTW performance, thus leading to a suboptimal WTW performance. To elucidate whether the RON requirement indeed affects the WTW performance, we perform the WTW optimization twice: once with a RON requirement of 110, and once with a RON requirement of only 90. We refer to these as RON 110+ and RON 90+ blends in the following. Figure 2 shows the WTW performance of both fuel types. Comparing the cost-optimal designs, the RON 90+ fuels exhibit both lower cost and GWI than the RON 110+ fuels, as along the whole Pareto front the trade-off between cost and GWI is favorable for the RON 90+ fuels. Comparing the GWI-optimal designs, the RON 90+ fuels exhibit a similar GWI but lower cost than the RON 110+ fuel.

The RON 110+ fuels contain ethanol, ethyl acetate, methyl acetate, and 2-MTHF, and a small fraction of *n*-pentane. Notably, the ethyl acetate content is highest at the cost-optimal design and decreases along the Pareto front toward the lowest GWI design. In contrast, the methyl acetate content is highest in the GWI-optimal design and decreases toward the cost-optimal design. Compared to the RON 110+ fuels, the RON 90+ fuels omit ethyl acetate and contain methanol, *n*-hexane, and *n*-pentane as additional fuel constituents. Furthermore, the methyl acetate content is reduced, whereas the alcohol, 2-MTHF, and hydrocarbon contents are increased. At lower cost, the ethanol content is very high; at lower GWI, the methyl acetate content is very high.

The changes in fuel composition with regard to the RON requirement can be explained as follows: Methyl and ethyl acetate enable meeting the RON requirement of the RON 110+ fuels, with RON values of 120 and 118, respectively. However, methyl acetate is synthesized from methanol (RON 108), and ethyl acetate is synthesized from ethanol (RON 109). Using the esters thus introduces further production costs and emissions compared to using the respective alcohols. The upgrading leads to an increase in engine efficiency, which, however does not always offset the additional cost and emissions of the production. Notably, at the GWI-optimal point, the RON 90+ fuel composition resembles the RON 110+ fuel composition, only the ethyl acetate fraction is replaced by higher shares of ethanol, 2-MTHF, and 1-hexene. Since the cost is not optimized here, the higher engine efficiency enabled by methyl acetate contributes to the better WTW performance. With decreasing cost, the RON 90+ fuels achieve a lower engine efficiency and compensate for the esters with higher concentrations in alcohols, 2-MTHF, and hydrocarbons compared to the RON 110+ fuels.

Overall, the results show that a very high RON requirement can impair the WTW performance. While the RON 110+ fuels achieve higher engine efficiencies, the superior TTW performance does not compensate the worse WTT performance. However, the TTW performance of our WTW-optimal fuels is superior to the TTW performance of RON 95 gasoline, as the RON 90+ fuels exhibit RON values ranging from 97 to 108 and allow for compression ratios from 12.3 to 15 and boost pressures up to 1.7 bar, resulting in relative engine efficiency increases of 4 to 11% compared to RON 95 gasoline. Hence, advanced SI engines still contribute to the WTW performance of the WTW-optimal alternative fuels by improving the TTW performance.

We note that instead of the simultaneous WTW design, the WTW performance could be optimized in a sequential fashion, i.e., by applying the WTT method[23] and subsequently optimizing the engine for the obtained fuel composition. In the Supporting Information, we show that the sequential optimization leads to fuels that are similar with respect to WTW performance and composition.

Results: Comparison to Drop-In Fuels

Neither the RON 90+ nor the RON 110+ fuels constitute drop-in fuels, i.e., they cannot be used to defossilize the operation of the current vehicle fleet. Apart from requiring new vehicles, these fuels would require establishing new fuel standards and modifications to the fuel distribution infrastructure. Obviously, such changes require a compelling argument, such as a significant improvement in cost and/or GWI.

We compare the RON 90+ and RON 110+ fuels to drop-in fuels based on the same process superstructure. To design these drop-in fuel candidates, we limit the allowable fuel constituents to the those specified in the European E10 standard,[37] i.e., hydrocarbons (synthetic gasoline from the MtG process, toluene, cyclopentane, *n*-pentane, *n*-hexane, 1-hexene), alcohols (methanol, ethanol), and ethers (2-MTHF). Further oxygenates such as ketones and esters are not allowed and are thus excluded. We furthermore fix the engine configuration to ε_{CR} = 10.4 and p_{in} = 1 bar, which is the optimal engine configuration for gasoline in the engine model.

https://doi.org/10.1021/acs.energyfuels.5c05792
Energy Fuels 2026, 40, 4207−4215

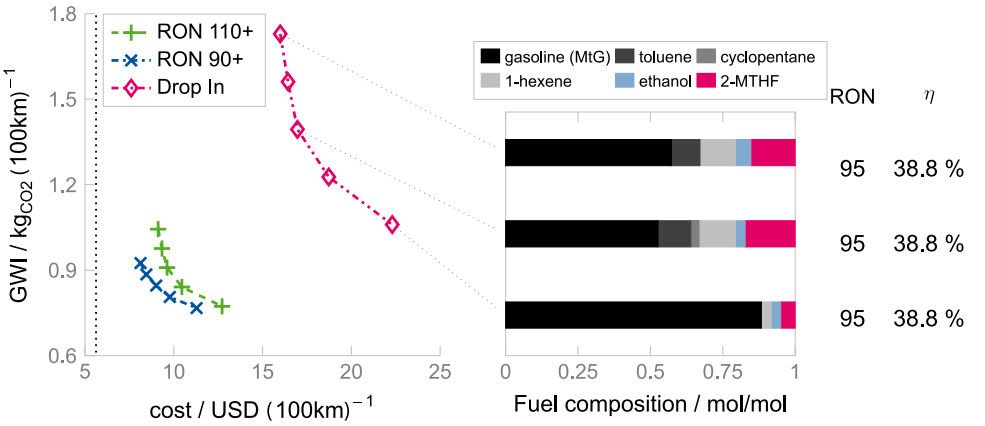

Figure 3. Comparison of well-to-wheel optimized fuels for ultrahigh efficiency engines with well-to-wheel optimized drop-in fuels. The black dotted line indicates the well-to-wheel cost of fossil gasoline. The black bars in the center plot represent a synthetic gasoline mixture obtained from the methanol-to-gasoline (MtG) process. The predicted RON and engine efficiency η are stated on the right. Note that the engine efficiency was evaluated using an engine configuration optimized for gasoline to emulate a currently used vehicle.

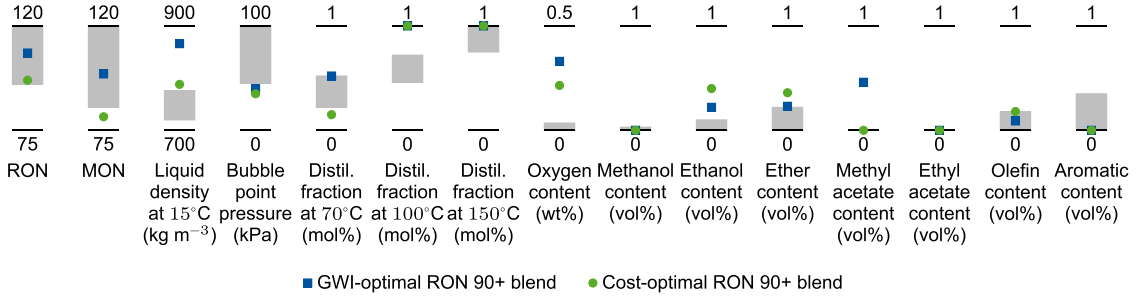

Figure 4. Comparison of the properties of the GWI and cost-optimal RON 90+ blends with respect to the specifications in the European E10 standard (gray areas). The numbers on the top and bottom of each bar denote the values used for normalization.

The Pareto front for the drop-in fuels is shown in Figure 3, along with the Pareto fronts of the RON90+ and RON 110+ fuels. The drop-in fuels yield costs of 16 to 22 $/100km and GWIs of 1.1 to 1.7 kg_{CO_2}/100km. When comparing the cost-optimal fuels, the RON 110+ fuel would achieve a cost reduction of 43% compared to the drop-in fuel. The RON 90+ fuel would achieve a cost reduction of 50%. When comparing the GWI-optimal fuels, the RON110+ fuel would achieve a GWI reduction of 27%, the RON 90+ fuel a GWI reduction of 28% compared to the drop-in fuel. We furthermore compare the results against the cost of fossil gasoline (5.6 $/100km[48]). While the drop-in fuels exhibit costs that are 200 to 300% higher than that of fossil gasoline, the RON 110+ fuels exhibit costs that are 60 to 130% higher, and the RON 90+ fuels exhibit cost that are only 40 to 100% higher. All renewable fuels exhibit significantly lower GWIs than fossil gasoline, as they are produced from renewable resources using a fully renewable energy system: the drop-in fuels would enable GWI reductions of 92 to 95%, where as the RON 90+ and RON 110+ fuels would enable GWI reductions of up to 96%.

Instead of designing a fuel complying with the current fuel standard, the fuel standard might be modified to enable the use of a more efficient renewable fuel. To evaluate such a scenario, we compare the properties of two RON 90+ blends with the ranges allowed in the European E10 standard (cf. Figure 4). The two fuels selected for the comparison are the cost and the GWI-optimal RON 90+ blend. Both fuels violate the specifications on liquid density, bubble point pressure, the distillation curve, the oxygen content, ethanol and ether contents. Furthermore, the cost-optimal fuel violates the MON specification, whereas the GWI-optimal fuel contains methyl acetate, an oxygenated species not allowed according to the fuel standard.

The most notable difference between both fuels is, however, the magnitude in which they deviate from the E10 specification. Most properties of the cost-optimal fuel only deviate slightly from the specifications. However, the fuel does not contain a component with a boiling point greater than or equal to 100 °C, whereas the standard specifies a maximum fuel fraction of 72 vol % to be evaporated at 100 °C. Moreover, with an ethanol content of 40 vol % and an ether content of 36 vol %, the blend exceeds the allowed oxygen content by a large margin. The high oxygen content can be expected to be incompatible with the current fleet, however, retrofitting vehicles might be a viable option and has been demonstrated for the use of liquefied petroleum gas[49] or ethanol-gasoline blends.[50] The GWI-optimal blend deviates more strongly in terms of liquid density and oxygen content, and furthermore exhibits a high fraction of methyl acetate, a component that is not allowed at all in the E10 standard.

Overall, the results implicate that drop-in fuels would exhibit both higher costs and higher GWIs than fuels that are not designed to be compatible with the current fleet and fuel standards. Retrofitting vehicles for these fuels, if possible, might be a more economically viable option. However, the comparison is limited to the possible fuel constituents and production processes included in the superstructure, which was developed for the early stage evaluation of highly selective processes. In the case of MtG, energy demands from a

https://doi.org/10.1021/acs.energyfuels.5c05792
Energy Fuels 2026, 40, 4207−4215

conceptual process design study were readily available, and the product mixture is assumed to resemble gasoline.

CONCLUSIONS

This article presents a first approach for model-based design of WTW optimal renewable fuels. Specifically, we optimize the WTW performance, i.e., the cost and GWI per distance driven, by considering a well-to-tank superstructure model and a tank-to-wheel model relying on a surrogate model of an advanced SI engine. In contrast to WTT fuel design approaches, our approach allows to consider the influence of the engine efficiency and thus forgoes the need to set a RON requirement.

We use the WTW design to examine the influence of different RON requirements on the WTW performance. The comparison of RON 90+ and RON 110+ fuels shows that permitting RON values lower than 110 leads to a superior well-to-wheel performance in our study. Still, the WTW-optimal fuels would require advanced SI engines to take advantage of engine efficiency increases enabled by their high knock resistance (RON $\geq$ 97). These fuels do not constitute drop-in fuels, i.e., they require changes in fuel infrastructure and vehicle fleet, as they do not meet fuel specifications derived from the E10 standard and contain esters and high concentrations of alcohols which may not be compatible with all materials used in the current infrastructure for fuel handling and the current cars. Drop-in fuels designed with the same process superstructure perform significantly worse than the RON 90+ and RON 110+ fuels. However, given the focus of the process superstructure on selective processes for oxygenated fuel constituents, these findings should not be generalized.

While the WTW optimization substantially improves upon previous integrated fuel and process design approaches, it also bears limitations. As in previous fuel design studies using the same WTT model, convergence to the global optimum could not be proven. To solve this issue, the optimization problem should be tested with different formulations and solvers, e.g., by deriving a reduced space formulation and solving the optimization problem with MAiNGO.[34] Although the engine model is validated against experiments covering multiple fuels and engine configurations, it is subject to considerable model uncertainties.[17] Moreover, the extrapolation from peak efficiency in a single-cylinder research engine to energy consumption of a vehicle is simplistic and might overestimate the potential of efficiency improvements. These two limitations could be overcome by using more accurate engine models to train the surrogate ANN; likely a larger ANN would be needed but the overall methodology may still be tractable. Given these uncertainties in the TTW performance, the uncertainties of the mixture properties caused by the use of mixing rules,[23] and the uncertainties of the WTT performance,[30] the designed blends should be refined in further stages of fuel development, by repeating the well-to-wheel optimization with more detailed models of production processes, fuel properties, engines, and vehicles. Furthermore, future work should include a broader range of unselective processes such as Fischer–Tropsch and hydrothermal liquefaction to elucidate whether alternative fuels generally exhibit a superior WTW performance compared to drop-in fuels.

ASSOCIATED CONTENT

Data Availability Statement

The model equations and data for process superstructure and fuel properties published in König et al.[23] and Panofen et al.[30] Additional data on MtG Process is listed in the Supporting Information. The code for the engine model is openly available in our GitLab repository "0D SI engine model for fuel design" at https://git.rwth-aachen.de/avt-svt/public/0d-si-engine-model-for-fuel-design, reference number.[51]

Supporting Information

The Supporting Information is available free of charge at https://pubs.acs.org/doi/10.1021/acs.energyfuels.5c05792.

> Brief description of the WTT model; Details on ignition delay time simulations, details on estimation of ignition delay time model parameters, list of all ignition delay time model parameters; Detailed report of errors of the engine surrogate model; Model of MtG process; Visualization of process superstructure used in the case study; Results of sequential WTW optimization (PDF)

AUTHOR INFORMATION

Corresponding Author

Manuel Dahmen − *Institute of Climate and Energy Systems−Energy Systems Engineering (ICE-1), Forschungszentrum Jülich GmbH, 52425 Jülich, Germany;* orcid.org/0000-0003-2757-5253; Email: m.dahmen@fz-juelich.de

Authors

Philipp Ackermann − *Process Systems Engineering (AVT.SVT), RWTH Aachen University, 52074 Aachen, Germany*

Marian Panofen − *Process Systems Engineering (AVT.SVT), RWTH Aachen University, 52074 Aachen, Germany;* orcid.org/0009-0008-6820-6925

Patrick Burkardt − *Chair of Thermodynamics of Mobile Energy Conversion Systems (TME), RWTH Aachen University, 52074 Aachen, Germany;* orcid.org/0000-0001-9433-4922

Bastian Lehrheuer − *Chair of Thermodynamics of Mobile Energy Conversion Systems (TME), RWTH Aachen University, 52074 Aachen, Germany*

Jörn Viell − *Process Systems Engineering (AVT.SVT), RWTH Aachen University, 52074 Aachen, Germany;* orcid.org/0000-0003-0587-6151

Stefan Pischinger − *Chair of Thermodynamics of Mobile Energy Conversion Systems (TME), RWTH Aachen University, 52074 Aachen, Germany; JARA-ENERGY, 52056 Aachen, Germany*

Alexander Mitsos − *Process Systems Engineering (AVT.SVT), RWTH Aachen University, 52074 Aachen, Germany; Institute of Climate and Energy Systems−Energy Systems Engineering (ICE-1), Forschungszentrum Jülich GmbH, 52425 Jülich, Germany; JARA-ENERGY, 52056 Aachen, Germany;* orcid.org/0000-0003-0335-6566

Complete contact information is available at: https://pubs.acs.org/10.1021/acs.energyfuels.5c05792

https://doi.org/10.1021/acs.energyfuels.5c05792
Energy Fuels 2026, 40, 4207−4215

Author Contributions

P.A. and M.D. formulated the research gap and scope of the study with conceptual input from M.P., B.L., J.V., S.P., and A.M. P.A. derived the surrogate model and energy consumption correlation, implemented the TTW model, conducted the optimizations, and analyzed the results with conceptual input from M.D., P.B., and B.L. M.P. provided the WTT code, performed the uncertainty quantification and network reduction, and provided conceptual input for the solution strategy. A.M., J.V., S.P., and B.L. supervised the project. P.A. wrote the original draft. All authors reviewed and edited the manuscript and gave their comments for improvements.

Notes

The authors declare no competing financial interest.

■ ACKNOWLEDGMENTS

The authors gratefully acknowledge funding by the Deutsche Forschungsgemeinschaft (DFG, German Research Foundation) under Germany's Excellence Strategy - Cluster of Excellence 2186 "The Fuel Science Center" ID: 390919832. AM and MD received funding from the Helmholtz Association of German Research Centers. An early version of this article was published in the first author's thesis,[52] Copyright by Philipp Ackermann.

■ REFERENCES

(1) Brusstar, M.; Stuhldreher, M.; Swain, D.; Pidgeon, W.; et al. High Efficiency and Low Emissions from a Port-Injected Engine with Neat Alcohol Fuels. *SAE Trans.* **2002**, *111*, 1445−1451.
(2) Verhelst, S.; Turner, J. W. G.; Sileghem, L.; Vancoillie, J. Methanol as a fuel for internal combustion engines. *Prog. Energy Combust. Sci.* **2019**, *70*, 43−88.
(3) Wouters, C.; Burkardt, P.; Pischinger, S. Limits of compression ratio in spark-ignition combustion with methanol. *Int. J. Engine Res.* **2022**, *23*, 793−803.
(4) Feng, H.; Lai, K.; Zheng, Z.; Lin, S.; Wu, X.; Tang, Q. Effects of methanol direct injection and high compression ratio on improving the performances of a spark-ignition passenger car engine. *Fuel* **2024**, *357*, No. 130052.
(5) Larsen, U.; Johansen, T.; Schramm, J. https://www.osti.gov/etdeweb/biblio/21580860 (accessed August 29, 2024).
(6) Johnson, T.; Joshi, A. Review of Vehicle Engine Efficiency and Emissions. *SAE Int. J. Engines* **2018**, *11*, 1307−1330.
(7) Dunn, J. B.; Newes, E.; Cai, H.; Zhang, Y.; Brooker, A.; Ou, L.; Mundt, N.; Bhatt, A.; Peterson, S.; Biddy, M. Energy, economic, and environmental benefits assessment of co-optimized engines and bio-blendstocks. *Energy Environ. Sci.* **2020**, *13*, 2262−2274.
(8) Dahmen, M.; Marquardt, W. Model-Based Design of Tailor-Made Biofuels. *Energy Fuels* **2016**, *30*, 1109−1134.
(9) McCormick, R. L.; Fioroni, G.; Fouts, L.; Christensen, E.; Yanowitz, J.; Polikarpov, E.; Albrecht, K.; Gaspar, D. J.; Gladden, J.; George, A. Selection Criteria and Screening of Potential Biomass-Derived Streams as Fuel Blendstocks for Advanced Spark-Ignition Engines. SAE. *Int. J. Fuels Lubr.* **2017**, *10*, 442−460.
(10) Rittig, J. G.; Ritzert, M.; Schweidtmann, A. M.; Winkler, S.; Weber, J. M.; Morsch, P.; Heufer, K. A.; Grohe, M.; Mitsos, A.; Dahmen, M. Graph Machine Learning for Design of High-Octane Fuels. *AIChE J.* **2023**, *69*, No. e17971.
(11) Kashinath, S. A. A.; Manan, Z. A.; Hashim, H.; Alwi, S. R. W. Design of green diesel from biofuels using computer aided technique. *Comput. Chem. Eng.* **2012**, *41*, 88−92.
(12) Kalakul, S.; Zhang, L.; Fang, Z.; Choudhury, H. A.; Intikhab, S.; Elbashir, N.; Eden, M. R.; Gani, R. Computer aided chemical product design − ProCAPD and tailor-made blended products. *Comput. Chem. Eng.* **2018**, *116*, 37−55.
(13) Kalghatgi, G. T. Fuel Anti-Knock Quality - Part I. Engine Studies. *SAE Trans.* **2002**, 1993−2004.
(14) Kuzhagaliyeva, N.; Horváth, S.; Williams, J.; Nicolle, A.; Sarathy, S. M. Artificial intelligence-driven design of fuel mixtures. *Commun. Chem.* **2022**, *5*, No. 111.
(15) Szybist, J. P.; Busch, S.; McCormick, R. L.; Pihl, J. A.; Splitter, D. A.; Ratcliff, M. A.; Kolodziej, C. P.; Storey, J. M.; Moses-DeBusk, M.; Vuilleumier, D.; Sjöberg, M.; Sluder, C. S.; Rockstroh, T.; Miles, P. What fuel properties enable higher thermal efficiency in spark-ignited engines? *Prog. Energy Combust. Sci.* **2021**, *82*, No. 100876.
(16) Gschwend, D.; Soltic, P.; Wokaun, A.; Vogel, F. Review and Performance Evaluation of Fifty Alternative Liquid Fuels for Spark-Ignition Engines. *Energy Fuels* **2019**, *33*, 2186−2196.
(17) Ackermann, P.; Auer, B.; Burkardt, P.; Lehrheuer, B.; Morsch, P.; Heufer, K. A.; Pischinger, S.; Mitsos, A.; Dahmen, M. Computational Co-Optimization of Fuel and Spark-Ignition Engine. *Energy Fuels* **2025**, *39*, 4079−4093.
(18) Marvin, W. A.; Rangarajan, S.; Daoutidis, P. Automated Generation and Optimal Selection of Biofuel-Gasoline Blends and Their Synthesis Routes. *Energy Fuels* **2013**, *27*, 3585−3594.
(19) Ng, L. Y.; Andiappan, V.; Chemmangattuvalappil, N. G.; Ng, D. K. A systematic methodology for optimal mixture design in an integrated biorefinery. *Comput. Chem. Eng.* **2015**, *81*, 288−309.
(20) Dahmen, M.; Marquardt, W. Model-Based Formulation of Biofuel Blends by Simultaneous Product and Pathway Design. *Energy Fuels* **2017**, *31*, 4096−4121.
(21) König, A.; Neidhardt, L.; Viell, J.; Mitsos, A.; Dahmen, M. Integrated design of processes and products: Optimal renewable fuels. *Comput. Chem. Eng.* **2020**, *134*, No. 106712.
(22) Restrepo-Flórez, J. M.; Maravelias, C. T. Advanced fuels from ethanol−a superstructure optimization approach. *Energy Environ. Sci.* **2021**, *14*, 493−506.
(23) König, A.; Siska, M.; Schweidtmann, A. M.; Rittig, J. G.; Viell, J.; Mitsos, A.; Dahmen, M. Designing Production-Optimal Alternative Fuels for Conventional, Flexible-Fuel, and Ultra-High Efficiency Engines. *Chem. Eng. Sci.* **2021**, *237*, No. 116562.
(24) Zhang, B.; Sarathy, S. M. Lifecycle optimized ethanol-gasoline blends for turbocharged engines. *Appl. Energy* **2016**, *181*, 38−53.
(25) Leone, T. G.; Anderson, J. E.; Davis, R. S.; Iqbal, A.; Reese, R. A.; Shelby, M. H.; Studzinski, W. M. The Effect of Compression Ratio, Fuel Octane Rating, and Ethanol Content on Spark-Ignition Engine Efficiency. *Environ. Sci. Technol.* **2015**, *49*, 10778−10789.
(26) Zuccari, F.; Orecchini, F.; Santiangeli, A.; Suppa, T.; Ortenzi, F.; Genovese, A.; Pede, G. Well to Wheel Analysis and Comparison Between Conventional, Hybrid and Electric Powertrain in Real Conditions of Use. In *74th ATI National Congress*; Cantore, G.; Allesina, G.; Pedrazzi, S.; Rinaldini, C. A., Eds.; AIP Publishing, 2019; p 020158.
(27) Khajavirad, A.; Sahinidis, N. V. A hybrid LP/NLP paradigm for global optimization relaxations. *Math. Program. Comput.* **2018**, *10*, 383−421.
(28) Schweidtmann, A. M.; Mitsos, A. Deterministic Global Optimization with Artificial Neural Networks Embedded. *J. Optim. Theory Appl.* **2019**, *180*, 925−948.
(29) Livengood, J. C.; Wu, P. C. Correlation of Autoignition Phenomena in Internal Combustion Engines and Rapid Compression Machines. *Symp. Int. Combust.* **1955**, *5*, 347−356.
(30) Panofen, M.; Ackermann, P.; Viell, J.; Mitsos, A.; Dahmen, M. Uncertainty Quantification in Integrated Fuel and Process Design. *Energy Fuels* **2024**, *38*, 14743−14756.
(31) *General Algebraic Modeling System (GAMS) Version 48.2.0*; GAMS Development Corporation: Fair-fax, VA, USA, 2024.
(32) Haimes, Y. Y.; Lasdon, L. S.; Wismer, D. A. On a bicriterion formation of the problems of integrated system identification and system optimization. *IEEE Trans. Syst. Man Cybern.* **1971**, *1*, 296−297.

https://doi.org/10.1021/acs.energyfuels.5c05792
Energy Fuels 2026, 40, 4207−4215

(33) Drud, A. S. CONOPT—A Large-Scale GRG Code. *ORSA J. Comput.* **1994**, *6*, 207−216.
(34) Bongartz, D.; Najman, J.; Sass, S.; Mitsos, A. MAiNGO-McCormick-Based Algorithm For Mixed-integer Nonlinear Global Optimization EURO: Dublin, Ireland, 2018.
(35) Bongartz, D.; Mitsos, A. Deterministic global optimization of process flowsheets in a reduced space using McCormick relaxations. *J. Global Optim.* **2017**, *69*, 761−796.
(36) Kunde, C.; Méndez, R.; Kienle, A. Deterministic Global Optimization of Multistage Layer Melt Crystallization Using Surrogate Models and Reduced Space Formulations. In *Computer Aided Chemical Engineering: 32 European Symposium on Computer Aided Process Engineering*; Montastruc, L.; Negny, S., Eds.; Elsevier, 2022; Vol. *51*, pp 727−732.
(37) DIN German Institute for Standardization Automotive fuels - Unleaded petrol - Requirements and test methods; German version EN 228:2012+A1:2017, Berlin.
(38) DIN German Institute for Standardization Automotive fuels - Automotive ethanol (E85) fuel - Requirements and test methods; German version EN 15293:2018, Berlin.
(39) Schreiner, M. https://www.osti.gov/servlets/purl/5153421 (accessed November 29, 2024).
(40) Maitlis, P. M.; de Klerk, A. *Greener Fischer−Tropsch Processes for Fuels and Feedstocks* Wiley: Weinheim, Germany, 2013; pp 209−220.
(41) Ulonska, K.; Skiborowski, M.; Mitsos, A.; Viell, J. Early-stage evaluation of biorefinery processing pathways using process network flux analysis. *AIChE J.* **2016**, *62*, 3096−3108.
(42) Jones, S. B.; Zhu, Y. https://www.osti.gov/servlets/purl/962846-1mQCPi/ (accessed November 29, 2024).
(43) Phillips, S. D.; Tarud, J. K.; Biddy, M. J.; Dutta, A. https://www.osti.gov/biblio/1004790 (accessed November 29, 2024).
(44) Sarathy, S. M.; Kukkadapu, G.; Mehl, M.; Javed, T.; Ahmed, A.; Naser, N.; Tekawade, A.; Kosiba, G.; AlAbbad, M.; Singh, E.; Park, S.; Rashidi, M. A.; Chung, S. H.; Roberts, W. L.; Oehlschlaeger, M. A.; Sung, C.-J.; Farooq, A. Compositional effects on the ignition of FACE gasolines. *Combust. Flame* **2016**, *169*, 171−193.
(45) De Klerk, A. *Fischer−Tropsch Refining*; Wiley-VCH: Weinheim, 2011.
(46) Andersen, V. F.; Anderson, J. E.; Wallington, T. J.; Mueller, S. A.; Nielsen, O. J. Distillation Curves for Alcohol−Gasoline Blends. *Energy Fuels* **2010**, *24*, 2683−2691.
(47) *MATLAB version 9.8.0.1359463 (R2020a)*; The MathWorks Inc.: Natick, MA, USA, 2020.
(48) Weekly Oil Bulletin by the European Commission. https://energy.ec.europa.eu/data-and-analysis/weekly-oil-bulletin_en (accessed September 29, 2023).
(49) Bermúdez, V.; Ruiz, S.; Sanchis, E. J.; Conde, B. Assessment of exhaust raw emissions and aftertreatment performance in a retrofitted heavy duty-spark ignition engine operating with liquefied petroleum gas. *J. Cleaner Prod.* **2024**, *434*, No. 140139.
(50) Dinh, T.; Nguyen, K.; Pham, T.; Nguyen, V. Study on performance enhancement and emission reduction of used carburetor motorcycles fueled by flex-fuel gasoline-ethanol blends. *J. Chin. Inst. Eng.* **2020**, *43*, 477−488.
(51) Ackermann, P.; Auer, B.; Burkardt, P.; Morsch, P.; Lehrheuer, B.; Heufer, K. A.; Pischinger, S.; Mitsos, A.; Dahmen, M. Open source 0D SI engine model for fuel design. https://git.rwth-aachen.de/avt-svt/public/0d-si-engine-model-for-fuel-design.
(52) Ackermann, P. Design of Well-to-Wheel-Optimal Alternative Fuels, Dissertation. RWTH Aachen University, 2025.

https://doi.org/10.1021/acs.energyfuels.5c05792
Energy Fuels 2026, 40, 4207−4215